

Supplemental Material and Data

Mesothelin-specific Chimeric Antigen Receptor mRNA-Engineered T cells Induce Anti-Tumor Activity in Solid Malignancies

Gregory L. Beatty^{1,3}, Andrew R. Haas^{1, 2}, Marcela V. Maus^{1,3}, Drew A. Torigian^{1,5}, Michael C. Soulen^{1,5}, Gabriela Plesa¹, Anne Chew¹, Yangbing Zhao^{1,4}, Bruce L. Levine^{1,4,6}, Steven M. Albelda^{1,2}, Michael Kalos^{1,4}, Carl H. June^{1,4,6}

Affiliations:

¹Abramson Cancer Center; University of Pennsylvania, Philadelphia, PA

²Division of Pulmonary, Allergy, and Critical Care, Department of Medicine, Perelman School of Medicine, University of Pennsylvania, Philadelphia, PA

³Division of Hematology-Oncology, Department of Medicine, Perelman School of Medicine, University of Pennsylvania, Philadelphia, PA

⁴Department of Pathology and Laboratory Medicine, Perelman School of Medicine, University of Pennsylvania, Philadelphia, PA

⁵Department of Radiology, Perelman School of Medicine, University of Pennsylvania, Philadelphia, PA

⁶Abramson Family Cancer Research Institute, Perelman School of Medicine, University of Pennsylvania, Philadelphia, PA

Supplemental Results

Safety of RNA CARTmeso cell infusions

MPM patient 17510-105 experienced no adverse events on schedule 1. However, patient 17510-105 developed anaphylaxis shortly after receiving the 1st infusion on Schedule 2, which prompted a short intensive care unit admission and was considered as “definitely related” to CARTmeso cell treatment. The patient was resuscitated with full clinical recovery. Extensive laboratory investigation demonstrated evidence of systemic mast cell degranulation probably related to an IgE-mediated anti-murine response to the murine CARTmeso construct sequences (1). PDA patient 21211-101 was enrolled onto Schedule 3 with a course complicated by bacterial sepsis after receiving five doses of CARTmeso cells that was determined to be unrelated to study treatment. However, as a result of this event, the patient missed the 6th infusion of CARTmeso cells but subsequently resumed therapy and completed the remaining three intravenous infusions without adverse events. Five days after receiving the last CARTmeso cell infusion, the patient was diagnosed with a grade 4 jejunal obstruction and was pulsed with methylprednisolone for 24 hours followed by a rapid taper given the possibility that the event could be related to CARTmeso cell infusion. The patient recovered rapidly within 4 hours of receiving steroids and achieved a complete resolution of all symptoms. Given the timing of the reaction, this event was considered “possibly related” to treatment although known peritoneal spread of the patient's disease was also considered a likely cause. The patient then received intratumoral injection of CARTmeso cells on day +35 which was complicated several hours after infusion by the development of grade 3 abdominal pain that was transient and resolved spontaneously within 24 hours. The event was considered "possibly related” to treatment. The patient received a repeat intratumoral injection of CARTmeso cells 22 days later on day +57 without further adverse

events. After completing this treatment schedule and returning to standard-of-care chemotherapy with gemcitabine, the patient's performance rapidly declined consistent with disease progression which was primarily manifested by refractory malignant ascites. The patient returned for further CARTmeso cell therapy and received an intraperitoneal injection of CARTmeso cells on day +91 at the time of a large volume paracentesis. The patient tolerated the infusion without adverse events.

Humoral immune responses directed against CARTmeso cells

The anaphylactic reaction observed with patient 17510-105 prompted an investigation for the development of antibody responses directed against the murine-derived ScFv sequences present in the CARTmeso construct. The presence of IgG antibodies capable of recognizing the CARTmeso construct was examined using a flow cytometry assay in which serum from patients was applied to unmodified Jurkat cells or Jurkat cells engineered to express a CARTmeso or a control CART19 construct. IgG human anti-chimeric antibodies (HACA) were undetectable in all patients at baseline. For patient 17510-105, no HACA response was observed at approximately 4 weeks after completing Schedule 1 (Fig. S2). However, this patient later developed a human anti-mouse antibody (HAMA) response after receiving one CARTmeso infusion on Schedule 2 which was detected on day +141 as previously reported (1). HACA responses became detectable in PDA patient 21211-101 after completing Schedule 3 (day +64) (Fig. S2).

Supplemental Methods

General laboratory statement

Research sample processing, freezing, and laboratory analyses were performed in the Translational and Correlative Studies Laboratory at the University of Pennsylvania, which operates under principles of Good Laboratory Practice with established standard operating procedures and/or protocols for sample receipt, processing, freezing, and analysis. Assay performance and data reporting conforms to MIATA guidelines (2).

Study design

A phase I clinical trial (NCT01355965) was designed to evaluate the manufacturing feasibility and safety of mRNA transduced CARTmeso cells in patients with advanced MPM. Patients received 1×10^8 CARTmeso cells administered on day 0 followed by a second infusion with 1×10^9 CARTmeso cells administered on day 7 (Schedule 1, Fig. S1B). Safety was evaluated for a minimum of 1 month and in the absence of dose limiting toxicity (DLT), patients were eligible to receive additional dosing with 1×10^8 CARTmeso cells administered 3x/week for one week followed by one week of rest and then 1×10^9 CARTmeso cells administered 3x/week for one week (Schedule 2, Fig. S1B). Tumor response was assessed by computed tomography (CT) at 1 month, 3 months and 6 months according to modified Response Evaluation Criteria in Solid Tumors (RECIST) for malignant pleural mesothelioma (3, 4).

Under a compassionate use study and the under same IND used for the MPM patient, a patient with advanced PDA (21211-101) was consented to receive $3 \times 10^8/\text{m}^2$ CARTmeso cells (5.52×10^8 cells) administered 3x/week for three weeks followed by CT-guided intratumoral injection of 2×10^8 CARTmeso cells on days +35 and +57 (Schedule 3, Fig. S1B). Tumor response was assessed by CT imaging at 1 month and 3 months according to RECIST 1.1.

Safety assessments included incidence of treatment-related adverse events (AEs), according to the National Cancer Institute Common Terminology Criteria of Adverse Events version 4.0. Dose limiting toxicity (DLT) was defined as toxicity following dosing that was at least “possibly related” to CAR T cell infusion and met one of the following criteria: 1) any grade 3 or higher toxicity with the exception that in the compassionate use protocol grade 3 asymptomatic electrolytes, nausea, vomiting, diarrhea and fatigue were not considered DLT; 2) grade 3 or higher autoimmune toxicity including pericarditis, peritonitis, or pleuritis; or 3) grade 3 or higher allergic reaction or grade 2 allergic reactions in which symptoms reappear after repeat infusion. Feasibility to manufacture CARTmeso cells was determined by measuring electroporation efficiency, T cell purity, viability, and sterility.

CTL assay

Cytolytic activity of CAR T cells was analyzed using a flow cytometry-based cytotoxicity assay. T cells were isolated from normal healthy volunteers by magnetic cell sorting via negative selection using a Pan T cell Isolation Kit (Miltenyi Biotec Inc., Auburn, CA) and then expanded with CD3/CD28 magnetic beads in the presence of 30 U/mL IL-2 followed by cryopreservation. For the cytolytic assay, T cells were thawed, and allowed to recover overnight. The cells were then electroporated with CART19 or CARTmeso RNA and allowed to rest for 24 hours as previously described (5, 6). The level of CAR expression was routinely two logs above background for >90% of cells. Tumor cells were adhered to culture plates 24 hours prior to addition of CAR T cells at effector:target ratios of 1:3, 1:1, 3:1, and 10:1. After 18 hours, all cells were stained for EpCAM, CD45 and 7-AAD and analyzed by flow cytometry using a BD Fortessa (BD Immunocytometry systems) equipped with Violet (405 nm), Blue (488 nm), Green (532 nm), and Red (633 nm) lasers and appropriate filter sets for detection and separation of the

fluorescently-conjugated antibodies. Countbright beads (BD Biosciences) were added to normalize for the volume of sample analyzed by flow cytometry. Specific killing was determined by calculating the difference in the number of live EpCAM⁺ 7-AAD^{neg} tumor cells between cultures with and without CAR T cells: percentage experimental EpCAM⁺ 7-AAD^{neg} cells minus percentage EpCAM⁺ 7-AAD^{neg} target cells in cultures without added effector CAR T cells.

Human anti-chimeric antibody (HACA) detection

HACA was detected using a flow cytometry based assay. Jurkat cells (ATCC TIB-152) transduced with either a lentiviral CARTmeso construct or negative control CART19 construct were incubated with patient derived serum at a 1:500 dilution, followed by incubation with a FITC-conjugated goat anti-human IgG Fc specific F(ab')₂ reagent (Jackson ImmunoResearch). Data was collected on an Accuri C6 cytometer (BD Biosciences) equipped with blue (488) and red (633 nm) lasers and analyzed using C-Flow software analysis package (version 1.0.264.9, BD Accuri Cytometers).

Protoarray analysis

To evaluate the development of humoral immune responses following CARTmeso treatment, high-throughput serological analysis was performed using protoarrayTM technology (Life Technologies). Serum samples were diluted 1:500 for the Protoarray analysis, per manufacturer instructions. For protoarray analysis, Gpr files containing signal intensities were imported into ProtoArray Prospector Software (v5.2, Life Technologies) where a comparison file was generated for linear model normalized intensities and “hit” flags indicated presence of antibodies. For the 9,480 unique probes on the array, ratios were calculated for each post-therapy sample against the patient-matched baseline pre-therapy sample. Where a baseline was not available, the median MFI value for the plate was utilized. Ratios were calculated compared to

the median normalized intensity of the array. Median MFI for plates was as follows: 17510-105 (pre: 1,522, day +110: 1,287, day +144: 1,620), and 21211-101(pre: 431, day +42: 510). For each time-point examined, pairs with post/pre ratios >3 were further analyzed. This selected set was then compared to an independent dataset compiled from 15 protoarray chips that used sera obtained from non-CAR T cell treated patients with cancer. Sets where post-MFI values were comparable to the average MFI of the control set were excluded from further analysis.

Immunoblot analysis

To detect CAR T cell-induced humoral responses against tumor antigens, we performed immunoblotting against purified proteins and extracts from cell lines as previously described (7). Briefly, whole cellular lysates from cells or purified proteins, including SV40 large T antigen (Chimerx, Milwaukee, WI) and mesothelin (Raybiotech, Norcross, GA), were prepared, run on an SDS Page gel, transferred to nitrocellulose, and immunoblotted with patient serum (diluted at 1:1500) from time points before treatment, and 6 weeks to 6 months after treatment. Whole cellular lysates were obtained from 1) allogeneic MPM cell lines (i.e. REN, 208, 213, 302, 307, M30, and M60) derived from patient pleural fluid samples from previous clinical trials (7), 2) an established allogeneic PDA cell line (Panc-1, ATCC CRL1469), and 3) an autologous cell line derived from the ascites of patient 21211-101. Immunoblots were analyzed to detect the presence of new or markedly increased bands in a semi-quantitative manner. Multiple exposures of pre- and post-treatment blots were obtained. Comparisons were made based on exposures where the major bands detected were of equal intensity. Two independent blinded observers visually scanned each blot carefully to detect new bands in blots exposed to post-treatment serum or bands that appeared markedly increased. There was complete consensus between reviewers.

PET Data Acquisition and Analysis

In patient 21211-101, FDG uptake within tumor lesions, as a measure of metabolic activity, was detected on PET/CT imaging at baseline, 5 weeks, and 11 weeks after treatment. FDG PET/CT was performed after the patient had fasted for ≥ 6 hours and plasma glucose levels were determined to be < 200 mg/dl. Approximately 15 mCi of FDG were administered intravenously, and 3D PET images were acquired ~ 60 minutes later from skull base to mid thighs for the baseline and 1st post-treatment study, and from skull vertex to toes for the 2nd post-treatment study. Attenuation correction of PET images was performed utilizing rescaled low-dose CT. Image analysis was performed using a software package which implements an automatic adaptive thresholding method (ROVER, ABX, GmbH, Germany) to delineate FDG avid lesions and to estimate metabolically active volume (MAV) and mean standardized uptake value (SUV_{mean}) for individual lesions from PET datasets as previously described (8-10). For each tumor lesion, mean metabolic volumetric product (MVP_{mean}) was determined by multiplying metabolism by volume [i.e. $MVP_{\text{mean}} = SUV_{\text{mean}} \times MAV$]. Total MVP_{mean} , a quantitative measure of global disease burden, was determined by summing MVP_{mean} of all lesions. Total pancreas, peritoneal, and hepatic lesion MVP_{mean} , as a measure of organ-specific disease burden, was determined by summing MVP_{mean} of defined organ lesions separately.

Supplemental References

1. Maus MV, Haas AR, Beatty GL, Albelda SM, Levine BL, Liu X, et al. T cells expressing chimeric antigen receptors can cause anaphylaxis in humans. *Cancer Immunology Research*. 2013;1:1-6.
2. Britten CM, Janetzki S, Butterfield LH, Ferrari G, Gouttefangeas C, Huber C, et al. T cell assays and MIATA: the essential minimum for maximum impact. *Immunity*. 2012;37:1-2.
3. Byrne MJ, Nowak AK. Modified RECIST criteria for assessment of response in malignant pleural mesothelioma. *Ann Oncol*. 2004;15:257-60.
4. Vogelzang NJ, Rusthoven JJ, Symanowski J, Denham C, Kaukel E, Ruffie P, et al. Phase III study of pemetrexed in combination with cisplatin versus cisplatin alone in patients with malignant pleural mesothelioma. *J Clin Oncol*. 2003;21:2636-44.
5. Zhao Y, Moon E, Carpenito C, Paulos CM, Liu X, Brennan AL, et al. Multiple injections of electroporated autologous T cells expressing a chimeric antigen receptor mediate regression of human disseminated tumor. *Cancer research*. 2010;70:9053-61.
6. Barrett DM, Zhao Y, Liu X, Jiang S, Carpenito C, Kalos M, et al. Treatment of advanced leukemia in mice with mRNA engineered T cells. *Hum Gene Ther*. 2011;22:1575-86.
7. Stermn DH, Recio A, Carroll RG, Gillespie CT, Haas A, Vachani A, et al. A phase I clinical trial of single-dose intrapleural IFN-beta gene transfer for malignant pleural mesothelioma and metastatic pleural effusions: high rate of antitumor immune responses. *Clin Cancer Res*. 2007;13:4456-66.

8. Torigian DA, Lopez RF, Alapati S, Bodapati G, Hofheinz F, van den Hoff J, et al. Feasibility and performance of novel software to quantify metabolically active volumes and 3D partial volume corrected SUV and metabolic volumetric products of spinal bone marrow metastases on 18F-FDG-PET/CT. Hellenic journal of nuclear medicine. 2011;14:8-14.
9. Hofheinz F, Langner J, Petr J, Beuthien-Baumann B, Oehme L, Steinbach J, et al. A method for model-free partial volume correction in oncological PET. EJNMMI research. 2012;2:16.
10. Hofheinz F, Potzsch C, Oehme L, Beuthien-Baumann B, Steinbach J, Kotzerke J, et al. Automatic volume delineation in oncological PET. Evaluation of a dedicated software tool and comparison with manual delineation in clinical data sets. Nuklearmedizin. 2012;51:9-16.

Supplemental Table 1. Patient demographics.

Subject	Age/sex	Disease	Prior therapies	Co-morbidities	Sites of disease at enrollment	Total infusions received and route of administration
17510-105	81/M	Malignant pleural mesothelioma	Pemetrexed/carboplatin (10 cycles) Pemetrexed (17 months) Intrapleural adenovirus-IFN α gemcitabine	asthma	Bilateral pleura, mediastinal and peritoneal lymph nodes	2 iv infusions (cohort 1); 1 iv infusion (cohort 2); total of 3 iv infusions
21211-101	75/M	Pancreatic adenocarcinoma	Gemcitabine/cisplatin (3 cycles) Modified FOLFOX6 (9 cycles)	-DVT on LMWH -Abdominal infections -h/o AML s/p syngeneic BMT 5 yrs prior to enrollment	Abdominal mass, liver masses, peritoneal nodules, ascites, Right knee subcutaneous	8 iv infusions; 2 intratumoral injections; 1 intraperitoneal injection

IFN α : interferon alpha; DVT: deep venous thrombosis; LMWH: low molecular weight heparin; AML: acute myelogenous leukemia; BMT: bone marrow transplant; iv: intravenous

Supplemental Table 2. Treatment-related adverse events.

Patient ID	Adverse Event	Severity	Relation to Study Treatment¹	Study day (days)	Time since prior infusion (days)²
17510-105	Cardiac arrest	4	Definitely	42	0-1
	Respiratory failure	4	Definitely	42	0-1
	Disseminated Intravenous Coagulation	4	Definitely	42	0-1
	Cytokine release syndrome	4	Definitely	42	0-1
21211-101	Jejunal obstruction	4	Possibly	23	5
	Abdominal pain	3	Possibly	35	0-1
	Lymphocytosis	2	Possibly	22	4

¹Relationship to study treatment was defined as “not related”, “unlikely related”, “possibly related”, “probably related”, or “definitely related”. Adverse events that were “not related” are not shown; ²Time since prior infusion indicates time since last CARTmeso cell infusion. Events occurring within the first 24 hours following an infusion are listed as “0-1”.

Supplemental Table 3. Protoarray analysis of serum samples from mesothelioma patient 17510-105

			Pre-	Day+110		day +144	
Database ID	Ultimate ORF ID	Description		Intensity	Ratio post/pre	Intensity	Ratio post/pre
NM_031439.1	IOH5524	SRY (sex determining region Y)-box 7 (SOX7)	2,878	25,811	8.97	15,383	5.35
BC031262.1	IOH21607	catenin (cadherin-associated protein), alpha 1, 102kDa (CTNNA1)	3,570	23,769	6.66	32,949	9.23
BC017943.1	IOH12235	protein phosphatase 1, regulatory (inhibitor) subunit 1C (PPP1R1C)	1,522	9,650	6.34	19,969	13.12
BC059405.1	IOH40433	Transducin-like enhancer protein 4	8,288	48,437	5.84	47,451	5.73
NM_032117.1	IOH23109	Meiotic nuclear division protein 1 homolog	2,897	15,920	5.50	11,212	3.87
NM_005423.1	IOH21844	trefoil factor 2 (spasmolytic protein 1) (TFF2)	1,522	7,509	4.94	20,800	13.67
NM_152266.1	IOH13579	chromosome 19 open reading frame 40 (C19orf40)	4,032	19,761	4.90	12,514	3.10
NM_012086.1	IOH55731	General transcription factor 3C polypeptide 3	2,157	8,513	3.95	8,529	3.95
BC033748.1	IOH21858	pyridoxal-dependent decarboxylase domain containing 1 (PDXDC1)	2,369	9,137	3.86	15,939	6.73

NM_022110.2	IOH10458	FK506 binding protein like (FKBPL)	1,522	5,036	3.31	6,841	4.50
NM_007202.2	IOH10972	A kinase (PRKA) anchor protein 10 (AKAP10), nuclear gene encoding mitochondrial protein	1,522	13,140	8.64	1,620	1.06
BC007014.1	IOH7141	tumor necrosis factor, alpha-induced protein 8 (TNFAIP8)	2,067	10,151	4.91	3,975	1.92
NM_001945.1	IOH23272	heparin-binding EGF-like growth factor (HBEGF)	1,522	7,003	4.60	1,620	1.06
NM_024294.1	IOH5168	chromosome 6 open reading frame 106 (C6orf106), transcript variant 1	3,692	15,544	4.21	10,228	2.77
NM_020651.2	IOH26519	pellino homolog 1 (Drosophila) (PELI1)	18,724	59,960	3.20	32,356	1.73
BC036804.1	IOH56311	chromosome 9 open reading frame 95 (C9orf95), transcript variant 2, mRNA.	1,522	4,869	3.20	1,620	1.06
NM_152261.1	IOH10854	chromosome 12 open reading frame 23 (C12orf23)	4,755	15,016	3.16	10,595	2.23
NM_007111.2	IOH13752	transcription factor Dp-1 (TFDP1)	1,609	5,069	3.15	3,674	2.28
NM_020548.4	IOH39853	diazepam binding inhibitor (GABA receptor modulator, acyl-Coenzyme A binding protein) (DBI), transcript variant 1	3,024	9,512	3.15	7,611	2.52
NM_020168.3	IOH20961	p21(CDKN1A)-activated kinase 6	5,175	16,071	3.11	9,946	1.92

		(PAK6)					
BC004106.1	IOH5672	mediator complex subunit 6 (MED6)	3,189	6,188	1.94	22,447	7.04
BC040020.2	IOH26263	zinc finger protein 280B (SUHW2)	3,813	2,075	0.54	23,877	6.26
BC021189.2	IOH22437	cDNA clone IMAGE:4829245	5,646	3,236	0.57	34,292	6.07
NM_145041.1	IOH13199	transmembrane protein 106A (TMEM106A)	3,157	1,665	0.53	17,769	5.63
NM_001008917.1	IOH50160	Similar to RIKEN cDNA 2210021J22 (OTTHUMP00000028822).	1,943	1,287	0.66	9,545	4.91
BC035938.1	IOH26798	myelin oligodendrocyte glycoprotein (MOG)	1,863	4,072	2.19	8,041	4.32
BC017314.2	IOH14156	v-ets erythroblastosis virus E26 oncogene homolog 1 (avian) (ETS1)	2,489	1,980	0.80	10,325	4.15
NM_006597.3	IOH11329	heat shock 70kDa protein 8 (HSPA8), transcript variant 1	3,277	6,570	2.00	12,881	3.93
NM_033214.2	IOH60256	Glycerol kinase 2	1,522	1,287	0.85	5,692	3.74

¹Database ID is the National Center for Biotechnology Information (NCBI) Reference Sequence; ²Ultimate ORF ID is an identifier used to identify the cDNA clone containing the open reading frame for a specific gene; ³Description provides information about the target protein; ⁴Signal intensity is indicated for pre- and post- (day+110 and +144) CARTmeso cell infusion; ⁵Ratio post/pre describes the ratio of signal intensities from serum obtained pre- and post-CARTmeso cell infusion.

Supplemental Table 3. (continued).

			Pre-	Day+110		day +144	
Database ID	Ultimate ORF ID	Description		Intensity	Ratio post/pre	Intensity	Ratio post/pre
NM_002297.2	IOH40729	lipocalin 1 (tear prealbumin) (LCN1)	1,644	2,653	1.61	5,995	3.65
NM_020836.2	IOH4129	brain-enriched guanylate kinase-associated homolog (rat) (BEGAIN)	1,716	1,976	1.15	5,806	3.38
BC024194.2	IOH40195	3-hydroxymethyl-3-methylglutaryl-Coenzyme A lyase-like 1 (HMGCLL1)	2,133	1,287	0.60	6,980	3.27
XM_117451.4	IOH42239	PREDICTED: Homo sapiens hypothetical LOC402617 (LOC402617)	20,015	65,163	3.26	65,269	3.26
PV3186		protein kinase C, iota (PRKCI)	1,910	1,471	0.77	6,049	3.17
NM_003673.2	IOH13813	titin-cap (telethonin) (TCAP)	4,874	10,208	2.09	15,311	3.14
NM_004143.2	IOH5542	Cbp/p300-interacting transactivator 1	2,554	2,676	1.05	7,950	3.11
BC011936.1	IOH12777	mediator complex subunit 28 (MED28)	1,522	1,849	1.22	4,664	3.07

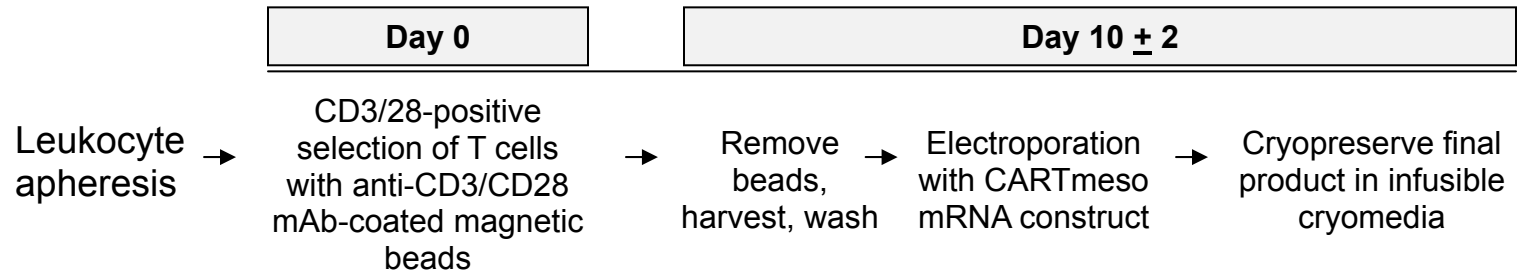
Supplemental Table 4. Protoarray analysis of serum samples from pancreatic cancer patient 21211-101.

Database ID	Ultimate ORF ID	Description	Pre-	day+44	
			Intensity	Intensity	Ratio post/pre
BC003548.1	IOH4864	polymerase (DNA directed), lambda (POLL)	564	62,437	110.70
NM_015129.3	IOH27517	septin 6 (SEPT6), transcript variant II	431	28,447	66.08
NM_003677.3	IOH56971	Density-regulated protein	431	18,521	43.02
NM_145802.1	IOH14040	septin 6 (SEPT6), transcript variant V	431	12,692	29.48
NM_033003.1	IOH5665	general transcription factor II, i (GTF2I), transcript variant 4	654	18,769	28.70
NM_053031.2	IOH59941	Myosin light chain kinase, smooth muscle	430	10,117	23.50
NM_015927.2	IOH3924	transforming growth factor beta 1 induced transcript 1 (TGFB1I1), transcript variant 2	687	15,098	21.98
NM_000431.1	IOH10122	Mevalonate kinase	2,517	49,352	19.61
NM_003315.1	IOH14566	DnaJ (Hsp40) homolog, subfamily C, member 7 (DNAJC7)	430	7,733	17.96
NM_006759.3	IOH26550	UDP-glucose pyrophosphorylase 2 (UGP2), transcript variant 1	697	12,385	17.78
XM_376764.2	IOH40703	paraneoplastic antigen MA2 (PNMA2)	1,759	27,277	15.51
NM_016954.2	IOH46151	T-box 22 (TBX22), transcript variant 2	430	6,653	15.45
BC012899.1	IOH11155	sialidase 4 (NEU4)	636	9,721	15.28

BC036846.1	IOH28739	protease, serine, 33 (PRSS33)	899	13,007	14.48
BC007637.1	IOH6973	chromosome 1 open reading frame 94 (C1orf94)	950	10,953	11.54
NM_024825.2	IOH29237	podocan-like 1, mRNA (cDNA clone MGC:71618 IMAGE:30347370), complete cds	430	4,865	11.30
BC000525.1	IOH3627	glutamic-oxaloacetic transaminase 2, mitochondrial (aspartate aminotransferase 2) (GOT2)	6,105	62,995	10.47
BC007560.1	IOH6825	LIM and SH3 protein 1 (LASP1)	431	4,295	10.00

¹Database ID is the National Center for Biotechnology Information (NCBI) Reference Sequence; ²Ultimate ORF ID is an identifier used to identify the cDNA clone containing the open reading frame for a specific gene; ³Description provides information about the target protein; ⁴Signal intensity is indicated pre- and post- (day+44) CARTmeso cell infusion; ⁵Ratio post/pre describes the ratio of signal intensities from serum obtained before and after CARTmeso cell infusion.

A



B

Schedule

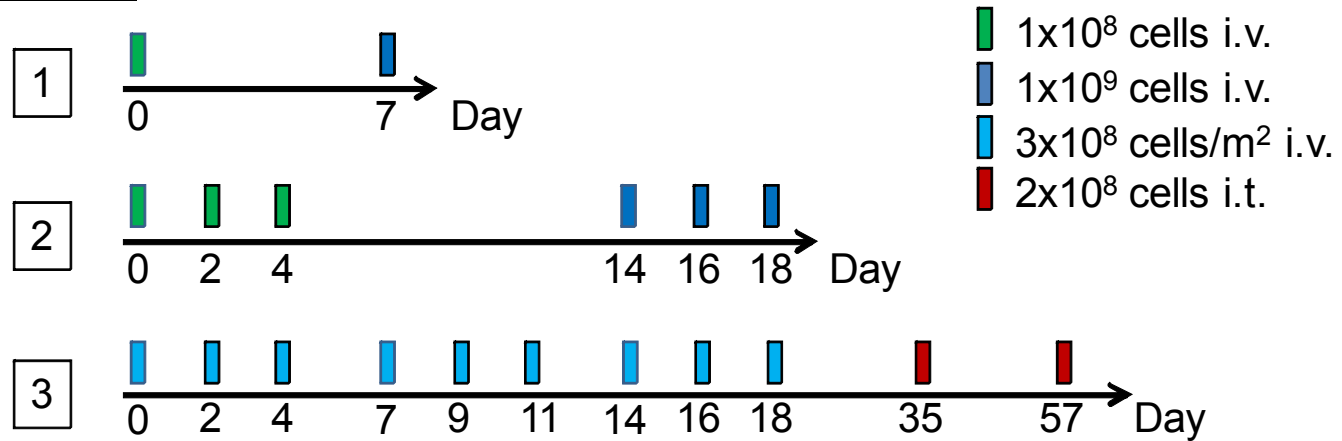


Figure S1. CARTmeso cell manufacturing and treatment schedules. (A) Autologous cells were obtained by leukocyte apheresis and T cells were enriched by expansion with anti-CD3/CD28 mAb coated magnetic beads. Cells were expanded for 8 to 12 days. On the last day of culture, the beads were removed using a magnetic field and the cells were washed, electroporated with CARTmeso mRNA construct, and cryopreserved in infusible medium. (B) Three treatment infusion schedules are being evaluated. On Schedule 1, patients receive 1×10^8 CARTmeso cells by intravenous (i.v.) infusion on day 0 followed by 1×10^9 CARTmeso cells one week later. Safety was monitored for a minimum of one month before patients were eligible for Schedule 2. On Schedule 2, patients receive 1×10^8 CARTmeso cells by i.v. infusion three times per week for one week followed by one week of rest and then 1×10^9 CARTmeso cells administered three times per week for one week. On Schedule 3, patients receive $3 \times 10^8/m^2$ CARTmeso cells by i.v. infusion three times per week for three weeks followed by intratumoral injection into the primary pancreas lesion of 2×10^8 CARTmeso cells on days +35 and +57.

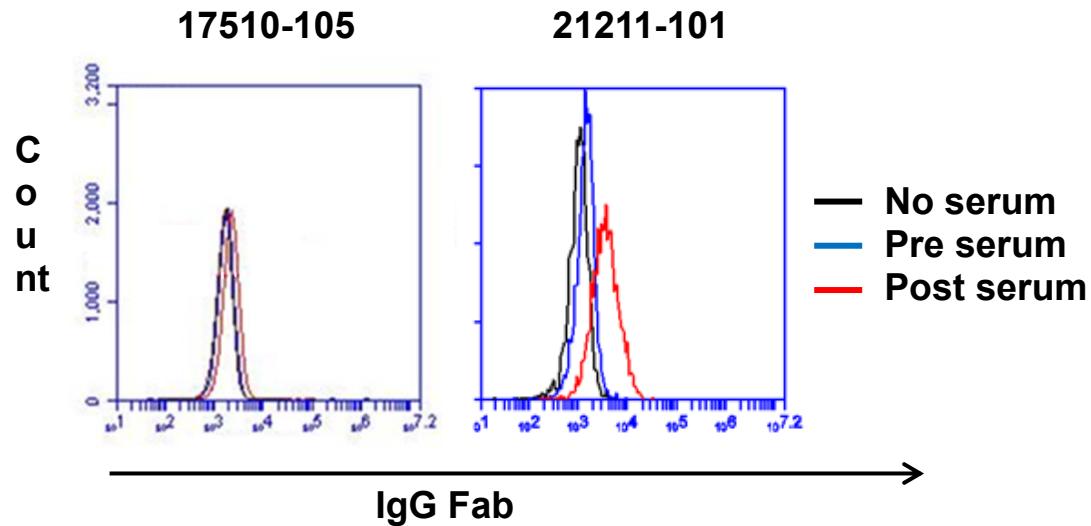


Fig S2. Detection of human anti-chimeric antibody responses in patients post-CARTmeso cell infusion. Sera collected from patients pre- and post-CARTmeso cell infusion were incubated with Jurkat cells engineered to express CARTmeso or CART19 and then analyzed by flow cytometry for the presence of HACA. A FITC-conjugated goat anti-human IgG Fc specific F(ab')₂ reagent was used for detection of anti-CART antibodies. In all cases, no antibody responses were detected when serum was incubated with Jurkat cells expressing CART19. Shown are histogram plots comparing the detection of antibody responses when serum obtained prior to CARTmeso cell infusion (Pre serum) and after infusion (Post serum) was incubated with Jurkat cells expressing CARTmeso. Post-serum time points for each patient are as follows: MPM 17510-105 – day +44; and PDA 21211-101 – day +64.

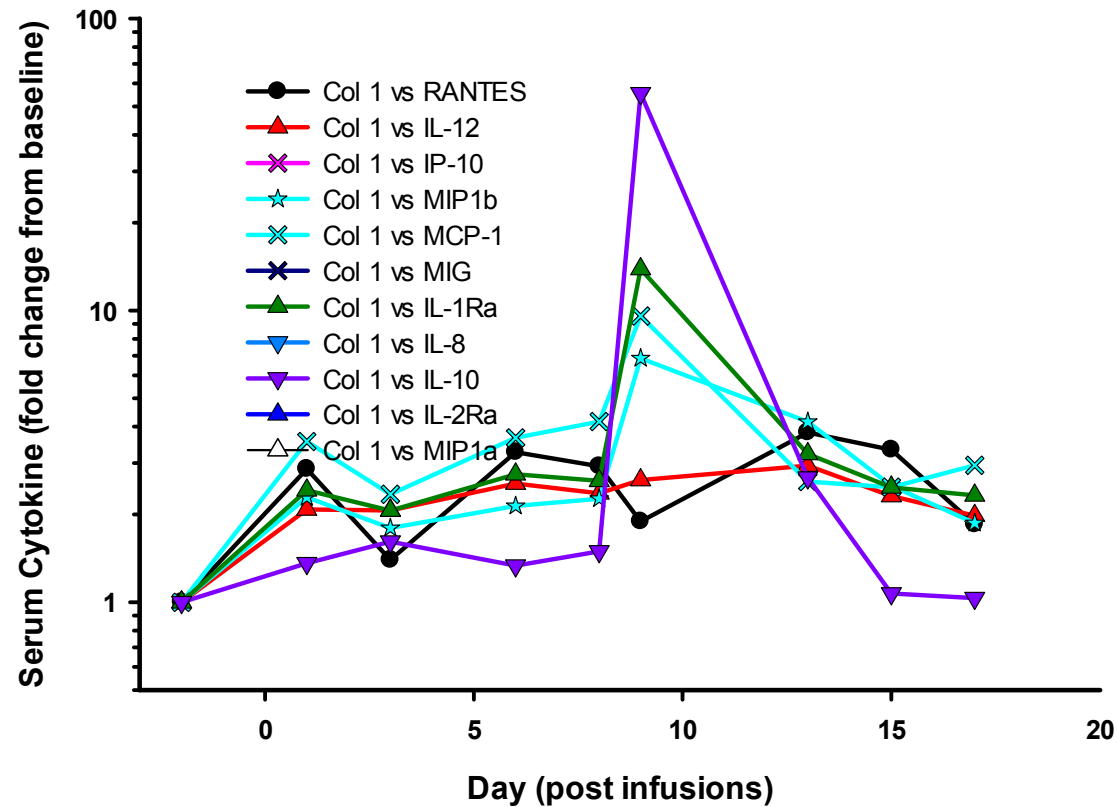


Fig S3. Serum cytokines and chemokines after CARTmeso cell infusion. The time course of the cytokines and chemokines shown for PDA patient 21211-101 in main text figure 3 are plotted. The fold change is plotted on the indicated day after first CAR T cell infusion. Baseline levels (pg/mL) of cytokines/chemokines were: IL-12, 58.0; IL-10, 1.3; RANTES, 2043; MIP-1Beta, 12.3; MCP-1 110.8; IL-1RA, 93.9. Of note, the cytokine burst at day 10 was in the setting of confirmed gram negative rod bacteremia with E coli and Enterobacter.

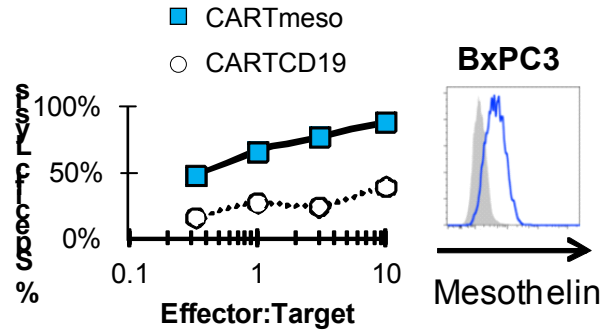
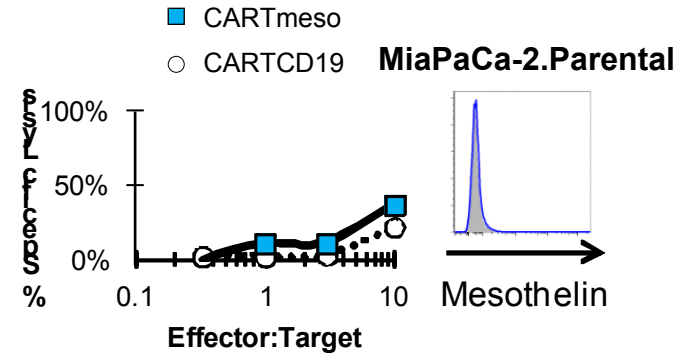
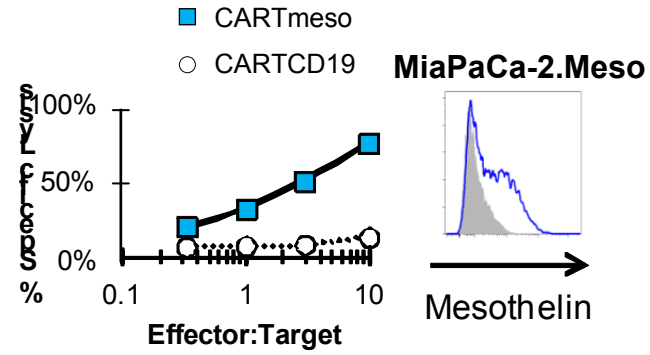
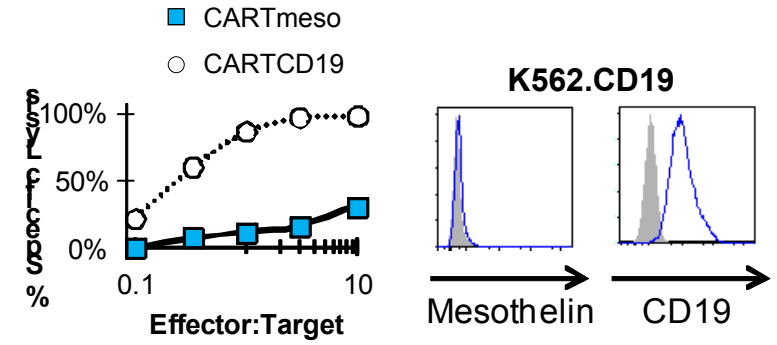
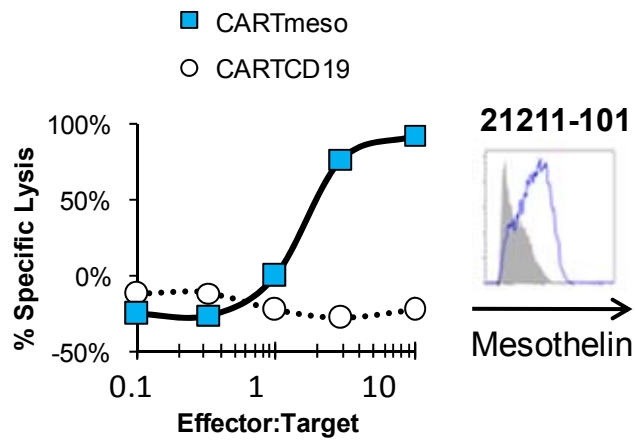
A**B****C****D****E**

Fig S4. CARTmeso cytolytic activity against allogeneic and autologous pancreatic cancer cell lines. (A-D) Allogeneic T cells from healthy volunteers or (E) autologous T cells used for treatment of PDA patient 21211 were electroporated with CARTmeso or CART19 RNA and used in a flow-cytometry based cytolytic assay with human pancreatic cancer cell lines. Shown is the percent specific lysis when CARTmeso or CART19 cells are incubated at varying E:T ratios with (A) BxPC3, (B) MiaPaCa-2, (C) MiaPaCa-2 transduced with mesothelin, (D) K562 transduced with CD19, and (E) a tumor cell line derived from the ascites of patient 21211. Histograms show cell line expression of mesothelin and CD19 expression as determined by flow cytometry.